

On the Energetic Stability and Electrochemistry of $\text{Li}_2\text{MnSiO}_4$ Polymorphs

M. E. Arroyo-deDompablo,^{*,†} R. Dominko,^{‡,§} J. M. Gallardo-Amores,[†] L. Dupont,^{||}
G. Mali,[‡] H. Ehrenberg,[⊥] J. Jamnik,[‡] and E. Morán[†]

Departamento de Química Inorgánica, Facultad de CC. Químicas, Universidad Complutense de Madrid, 28040 Madrid, Spain, National Institute of Chemistry, Hajdrihova 19, SI-1000 Ljubljana, Slovenia, ALISTORE European Research Institute, Amiens, France, LRCS, Université de Picardie Jules Verne, UMR 6007, 33 rue Saint-Leu, 80039, Amiens, France, and IFW Dresden, Helmholtzstrasse 20, D-01069 Dresden, Germany

Received April 15, 2008. Revised Manuscript Received June 22, 2008

The thermodynamic stability of $\text{Li}_2\text{MnSiO}_4$ polymorphs and their electrochemical properties as electrode for Li batteries are investigated combining experimental and computational methods. Three possible $\text{Li}_2\text{MnSiO}_4$ forms have been considered crystallizing in $Pmnb$, $Pmn2_1$ ($\beta\text{-Li}_3\text{PO}_4$ derivatives) and $P2_1/n$ ($\gamma\text{-Li}_3\text{PO}_4$ derivative) space groups (S.G.). We have first demonstrated that the relative stability of β - and $\gamma\text{-Li}_3\text{PO}_4$ polymorphs is well-reproduced by density functional theory (DFT) methods (LDA, GGA). For $\text{Li}_2\text{MnSiO}_4$, the $Pmnb$ form is predicted to be 2.4 meV/f.u. and 65 meV/f.u. more stable than the $Pmn2_1$ and $P2_1/n$ forms, respectively (GGA + U results). Computational results indicate that the denser $Pmn2_1$ polymorph can be obtained by high pressure/high temperature treatment of the other polymorphs or their mixtures. A sample of $\text{Li}_2\text{MnSiO}_4$ prepared at 900 °C consists of a mixture of polymorphs, as detected by XRD and confirmed by means of SAED and ^6Li MAS-NMR. As expected from DFT results, exposing the as-prepared $\text{Li}_2\text{MnSiO}_4$ sample to high pressure/high temperature (pressure range 2–8 GPa, temperature range 600–900°C) allows to isolate the $Pmn2_1$ polymorph. The crystal structure has a minor impact in the average lithium intercalation voltage for the two electron process (GGA+U calculated voltages are 4.18, 4.19, and 4.08 V for $Pmnb$, $Pmn2_1$ and $P2_1/n$, respectively). Major structural rearrangements are expected under lithium deinsertion from the $P2_1/n$ polymorph, as previously found for the $\beta\text{-Li}_3\text{PO}_4$ derivatives, rendering any MnSiO_4 delithiated hosts prompt to transform into a more stable structure or a mixture of them.

Introduction

The Li_2MSiO_4 (M = Fe, Mn, Co, Ni) family is attractive as positive electrode for lithium batteries due to its improved safety and at least theoretical possibility to reversibly deintercalate two lithium equivalents from the structure. The electrochemistry of $\text{Li}_2\text{FeSiO}_4$, $\text{Li}_2\text{MnSiO}_4$, and $\text{Li}_2\text{CoSiO}_4$ towards Li^+/Li has been reported showing that these compounds are able to provide one electron per formula unit at average voltages of ca. 3.1, 4.2, and 4.3V, respectively.^{1–4} Li_2MSiO_4 compounds crystallize in several different polymorphs. A recent work on $\text{Li}_2\text{FeSiO}_4$ ² found a structure of orthorhombic symmetry, related to the low-temperature form

of Li_3PO_4 ⁵ ($\beta\text{-Li}_3\text{PO}_4$) (Figure 1a), which can be described as built up from infinite corrugated layers of composition $[\text{SiMO}_4]_\infty$ lying on the *ac*-plane and linked along the *b*-axis by LiO_4 tetrahedra. Within these layers each SiO_4 tetrahedron shares its four corners with four neighboring MO_4 tetrahedra, and vice versa. Lithium ions also occupy tetrahedral sites located between two of the $[\text{SiMO}_4]_\infty$ layers, in such a way that a path for lithium motion (facilitating the extraction/insertion process) exists in the structure. So far this has been the only crystal structure reported for $\text{Li}_2\text{FeSiO}_4$. However, in the case of $\text{Li}_2\text{CoSiO}_4$, up to four different polymorphs have been prepared to date.^{4,6} Interestingly, all the $\text{Li}_2\text{CoSiO}_4$ polymorphs display similar electrochemical properties as positive electrode in Li cells.⁴ The case of $\text{Li}_2\text{MnSiO}_4$ is more puzzling.^{1,7} Dominko et al.¹ found a similar orthorhombic cell to that reported for $\text{Li}_2\text{FeSiO}_4$, electrochemically active at 4.12 V vs. Li, whereas Poliatev et al.⁷ prepared a monoclinic variety with a poor electrochemical response at an open circuit voltage of 3.76 V vs lithium.

In the view of a potential application of Li_2MSiO_4 (M = Fe, Mn, Co, Ni) and its solid solutions, it is relevant to clarify

* Corresponding author. E-mail: e.arroyo@quim.ucm.es.

† Universidad Complutense de Madrid.

‡ National Institute of Chemistry.

§ ALISTORE European Research Institute.

|| Université de Picardie Jules Verne.

⊥ IFW Dresden.

- (1) Dominko, R.; Bele, M.; Gaberscek, M.; Meden, A.; Remskar, M.; Jamnik, J. *Electrochem. Commun.* **2006**, 8 (2), 217–222.
- (2) Nyten, A.; Abouimrane, A.; Armand, M.; Gustafsson, T.; Thomas, J. O. *Electrochem. Commun.* **2005**, 7 (2), 156–160.
- (3) Yang, Y.; Li, Y.; Gong, Z. Presented at the 12th International Meeting on Lithium Batteries, June 13–18, Biarritz, France, 2006; The Electrochemical Society: Pennington, NJ, 2006; Abstract 210.
- (4) Lyness, C.; Delobel, B.; Armstrong, A. R.; Bruce, P. *Chem. Commun.* **2007**, 46, 4890–4892.

(5) Keffer, C.; Michell, A.; Mauer, F.; Swanson, H.; Block, S. *Inorg. Chem.* **1966**, 6 (1), 119–125.

(6) West, A. R.; Glasser, F. P. *J. Solid State Chem.* **1972**, 4, 20–28.

(7) Poliatev, V. V.; Petrenko, A. A.; Nalbandyan, V. B.; Medvedev, B. S.; Shvetsova, E. S. *J. Solid State Chem.* **2007**, 180, 1055–1060.

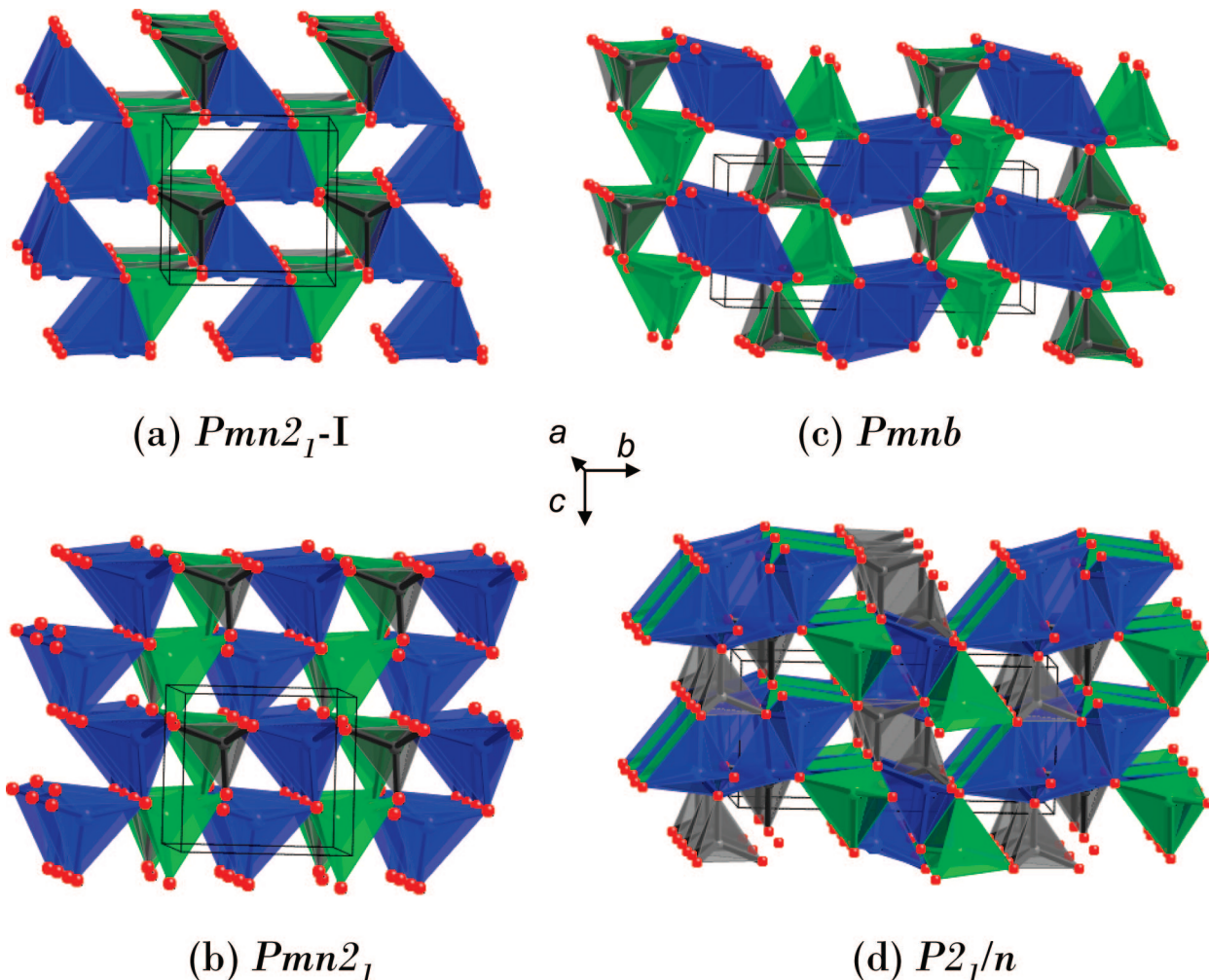


Figure 1. Schematic crystal structure of some possible $\text{Li}_2\text{MnSiO}_4$ polymorphs (a) $Pmn2_1$ -I from ref 2, (b) $Pmn2_1$ from ref 1, (c) $Pmnb$, and (d) $P2_1/n$. LiO_4 , MnO_4 , and SiO_4 tetrahedra are colored in blue, green, and gray, respectively. Oxygen atoms are denoted by red balls.

Table 1. Ground-State Structural Parameters for Li_3PO_4 Polymorphs Calculated within the DFT in Comparison with Experimental Values

	β - Li_3PO_4					γ - Li_3PO_4				
	calcd		exp ⁵	error %		calcd		exp ¹⁷	error %	
	GGA	LDA		GGA	LDA	GGA	LDA		GGA	LDA
<i>a</i>	6.164	5.989	6.115(1)	0.8	2.0	6.151	5.999	6.12	0.5	1.9
<i>b</i>	5.286	5.137	5.2394(11)	0.8	1.9	10.564	10.319	10.53	0.3	2.0
<i>c</i>	4.892	4.746	4.8554(10)	0.7	2.2	4.971	4.805	4.93	0.8	2.5
<i>V</i> (f.u.)	79.70	73.02	77.78	2.4	6.1	80.76	74.73	79.42	1.7	5.9

the thermodynamic stability of Li_2MSiO_4 polymorphs and to evaluate the influence of the crystal chemistry in their electrochemical performances. In this work, we focus on the polymorphs of $\text{Li}_2\text{MnSiO}_4$. By first principles methods, it is possible to calculate the total energy of any crystal structure, and hence to infer the relative stability of polymorphs from the difference of their calculated total energies. The usefulness of first principles methods to investigate the stability of crystal phases as a function of pressure has been demonstrated in many systems, such as hydrogen,⁸ V_2O_5 ,^{9,10}

MgSiO_3 ,¹¹ carbon,^{12,13} or SiO_2 .^{14,15} In this work, we present a density functional theory study of $\text{Li}_2\text{MnSiO}_4$ polymorphs, focusing on the relative thermodynamic stability of proposed crystal structures and their respective electrochemical properties. Polymorphism of Li_3PO_4 has also been computationally investigated for comparison. Furthermore, computational data are used to guide experiments towards the preparation of the different $\text{Li}_2\text{MnSiO}_4$ polymorphs.

Crystal Structures of Possible $\text{Li}_2\text{MnSiO}_4$ Polymorphs. Every reported Li_2MSiO_4 polymorph is related to either the low temperature form or the high temperature form

(8) Pickard, C. J.; Richard, J. N. *Nat. Phys.* **2007**, *3*, 473–476.

(9) Balog, P.; Orosel, D.; Cancarevic, Z.; Schön, C.; Jansen, M. *J. Alloys Compd.* **2007**, *429*, 87–98.

(10) Gallardo-Amores, J. M.; Biskup, N.; Amador, U.; Persson, K.; Ceder, G.; Moran, E.; Arroyo, y. de; Dompablo, M. E. *Chem. Mater.* **2007**, *19* (122), 5262–5271.

(11) Oganov, A. R.; Ono, S. *Nature* **2004**, *430*, 445–448.

(12) Galli, G.; Martin, R. M.; Car, R.; Parrinello, M. *Science* **1990**, *250*, 1547–1549.

(13) Grumbach, M. P.; Martin, R. M. *Phys. Rev. B* **1996**, *54*, 2471–2474.

(14) Bonev, S. A.; Gygi, F.; Ogitsu, T.; Galli, G.; *Phys. Rev. Letters* **2003**, *91*, 065501.

(15) Hamann, D. R. *Phys. Rev. Lett.* **1996**, *76* (14), 660–663.

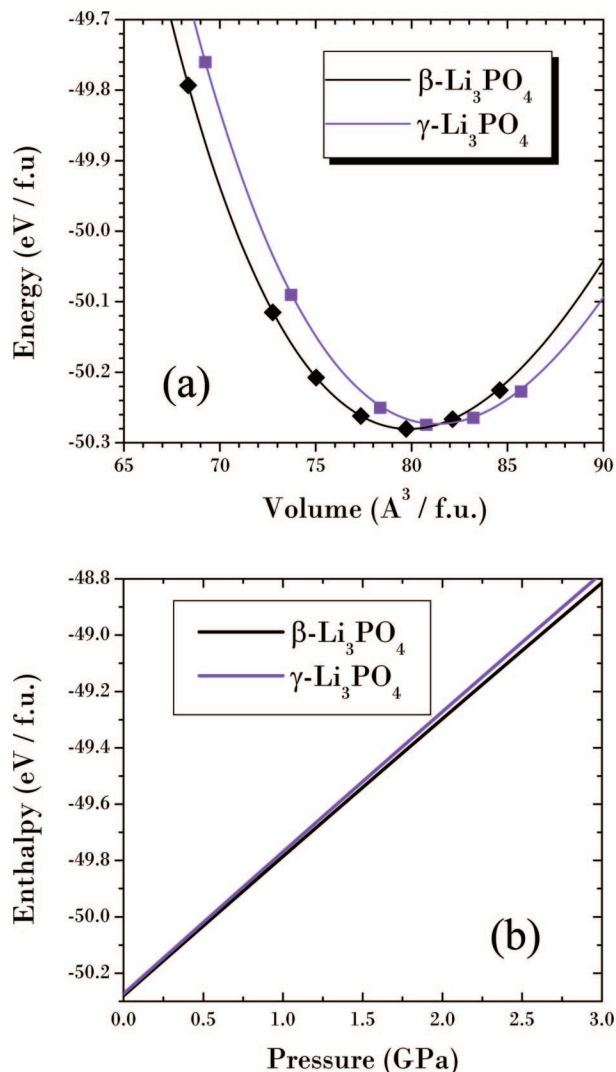


Figure 2. (a) Calculated total energy vs volume curves for $\beta\text{-Li}_3\text{PO}_4$ (black) and $\gamma\text{-Li}_3\text{PO}_4$ (violet). Symbols correspond to the DFT calculated data, and lines show the fitting to the Murnaghan equation of state. (b) Enthalpy per f.u. vs pressure for $\beta\text{-Li}_3\text{PO}_4$ (black) and $\gamma\text{-Li}_3\text{PO}_4$ (violet).

of Li_3PO_4 , denoted as $\beta\text{-Li}_3\text{PO}_4$ and $\gamma\text{-Li}_3\text{PO}_4$, respectively. $\beta\text{-Li}_3\text{PO}_4$ (S.G. $Pmn2_1$) presents a structure consisting of only corner-sharing tetrahedra, in which all the tetrahedra point towards the same orientation along the c axis.⁵ The structure found for $\text{Li}_2\text{FeSiO}_4$ (Figure 1a) crystallizes in the S.G. $Pmn2_1$, but clearly differs from that of $\beta\text{-Li}_3\text{PO}_4$ because the tetrahedra do not point to the same orientation, and each Si tetrahedron shares edges with two Li tetrahedra creating two very short Si–Li distances of 2.5 Å. This model will be denoted as $Pmn2_1\text{-I}$. The first model that was proposed for $\text{Li}_2\text{MnSiO}_4$ (Figure 1b) is isostructural with $\beta\text{-Li}_3\text{PO}_4$ and will be denoted simply as $Pmn2_1$. Another model proposed for $\text{Li}_2\text{MnSiO}_4$ (S.G. $Pmnb$)^{1,16} is shown in Figure 1c; along the b axis, two rows of Li tetrahedra connect the $[\text{MSiO}_4]$ layers by corner sharing. In this model (denoted as $Pmnb$) the b lattice parameter doubles with respect to that of the $Pmn2_1$ and $Pmn2_1\text{-I}$ cells. The presence of a two dimensional $[\text{SiMO}_4]$ skeleton, as in the above $Pmnb$ model, makes us consider this structure related to $\beta\text{-Li}_3\text{PO}_4$, even though the

two Li rows have common edges (Li–Li distance is 2.75), and tetrahedra pointing up and down along the c direction alternate in the structure. In the present work, we have studied these three $\beta\text{-Li}_3\text{PO}_4$ related structures. $\gamma\text{-Li}_3\text{PO}_4$ (S.G. $Pmnb$) is built by both corner- and edge-sharing tetrahedra and with half of the tetrahedra pointing to opposite orientations along the c axis than the other half.¹⁷ The fourth possible polymorph under investigation is the reported monoclinic $\text{Li}_2\text{MnSiO}_4$ ⁷ (S.G. $P2_1/n$, Figure 1d), a derivative of $\gamma\text{-Li}_3\text{PO}_4$, in which edges are shared between tetrahedral Li, with Li–Li distances of 2.7 Å. This structure comprises a three-dimensional $[\text{SiMO}_4]$ framework.

Methodology

Computational. The total energies of all the compounds under study were calculated using the Projector Augmented Wave (PAW)^{18,19} formalism as implemented in the Vienna Ab initio Simulation Package (VASP)²⁰ with the exchange and correlation energies approximated in the Generalized Gradient Approximation (GGA). In the case of Mn compounds, spin-polarized calculations were performed, also adding the Hubbard parameter correction (GGA+U) with a J term value of 1 eV and U value of 5 eV, because those have been recently reported as appropriated values for Mn^{2+} compounds.^{21,22} For the exchange and correlation functional we choose a form suggested by Perdew, Burke, and Ernzerhof (PBE).²³ The total energy of Li_3PO_4 polymorphs were also calculated within the Local Density Approximation (LDA) using ultrasoft pseudopotentials. The wave functions were expanded with a plane-wave basis set with a cut-off kinetic energy of 500 eV. The integration in the Brillouin zone is done by using the tetrahedron method as corrected by Blöchl on a set of k -points ($6 \times 6 \times 6$ for $Pmn2_1$ and $6 \times 4 \times 6$ for $Pmnb$, and $P2_1/n$) determined by the Monkhorst–Pack scheme. Using these parameters, we achieved a total-energy convergence close to 4 meV per formula unit. The initial cell parameters and atomic positions of $\beta\text{-Li}_3\text{PO}_4$ and $\gamma\text{-Li}_3\text{PO}_4$ were taken from refs 5 and 17, respectively. For $\text{Li}_2\text{MnSiO}_4$, initial structures respond to the models above described: $Pmn2_1\text{-I}$,² $Pmn2_1$,¹ $Pmnb$,¹⁶ and $P2_1/n$.⁷ In these computed models, we have considered the perfect structures, where no Mn substitutes for Li and vice versa. As a first step, the structures were fully relaxed (cell parameters, volume cells, and atomic positions); the final energies of the optimized geometries were recalculated so as to correct for the changes in the basis set of the wave functions during relaxation. Secondly, relaxed structure calculations were performed at various constant volumes and the energy–volume data were fitted to the Murnaghan equation of state.²⁴ Li ions were selectively removed from the $\text{Li}_2\text{MnSiO}_4$ optimized structures leading to MnSiO_4 compounds, the structures of which were also fully relaxed. We considered all the $\text{Li}_2\text{MnSiO}_4$ and MnSiO_4 crystal structures in a ferromagnetic configuration. Preparation and analysis of VASP files were done primarily with the CONVASP code.²⁵ Analysis of crystal symmetry was performed using the PLATON program.²⁶

(17) Zemann, J. *Acta Crystallogr., Sect. B* **1960**, *13*, 863.

(18) Bloch, P. E. *Phys. Rev. B* **1994**, *50*, 17953.

(19) Kresse, G.; Joubert, J. *Phys. Rev. B* **1999**, *59*, 1758.

(20) Kresse, G.; Furthmüller, J. *Comput. Mater. Sci.* **1996**, *15*, 6.

(21) Zhou, F.; Cococcioni, M.; Marianetti, C. A.; Morgan, D.; Ceder, G. *Phys. Rev. B* **2004**, *15*, 235121–1.

(22) Wang, L.; Maxisch, T.; Ceder, G. *Phys. Rev. B* **2006**, *73*, 1195107–1–195107–6.

(23) Perdew, J. P.; Burke, K.; Ernzerhof, M. *Phys. Rev. Lett.* **1996**, *77* (18), 3865–3868.

(24) Murnaghan, F. D. *Proc. Natl. Acad. Sci., U.S.A.* **1944**, *30*, 244.

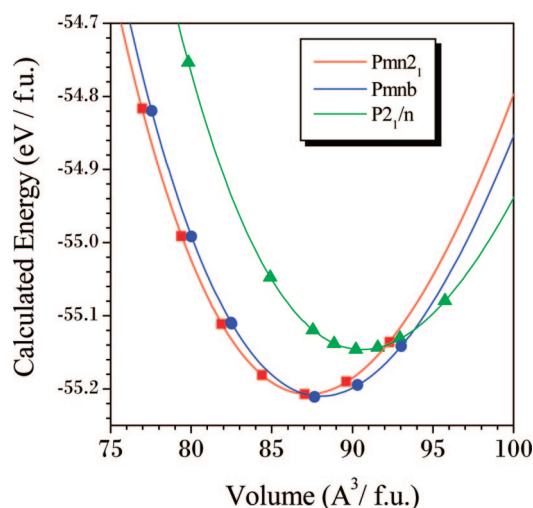
(16) Meden, A. In preparation

Table 2. Calculated Lattice Parameters for the Optimized Polymorphs of $\text{Li}_2\text{MnSiO}_4$ Confronted with the Experimental Data That Were Used As Initial Models of the Calculation

	$Pmn2_1$ -I ^{2a}		$Pmn2_1$ ¹		$Pmnb$ ¹⁶		$P2_1/n$ ⁷	
	opt	exp	opt	exp	opt	exp	opt	exp
<i>a</i>	6.370	6.2661(5)	6.366	6.3109(9)	6.356	6.30814(13)	6.390	6.3344(4)
<i>b</i>	5.436	5.3295(5)	5.433	5.3800(9)	10.873	10.75946(22)	11.010	10.9108(7)
<i>c</i>	5.027	5.0148(4)	5.032	4.9662(8)	5.073	5.00909(10)	5.130	5.0703(4)
β							91.06	90.990
<i>V</i> (f.u.)	87.04	83.72	87.03	84.30	87.65	84.99	90.22	87.7

^a Initial model is for $\text{Li}_2\text{FeSiO}_4$.**Table 3.** Calculated Bond Lengths for the Optimized Polymorphs of $\text{Li}_2\text{MnSiO}_4$; Data from the Initial Models Are Given for Comparison

	$Pmn2_1$ -I ²		$Pmn2_1$ ¹		$Pmnb$ ¹⁶		$P2_1/n$ ⁷	
	opt	initial ^a	opt	initial	opt	initial	opt	initial
Li–O	1.9563	1.7919	1.9584	1.9210	1.9540	1.8643	1.9494 (1.9373)	1.8981 (1.9168)
	1.9724	1.8528	1.9825	1.9282	1.9589	1.9485	1.9605 (1.9868)	1.9389 (1.9597)
	1.9995	1.9446	1.9896	2.0078	2.0065	1.9661	2.0198 (2.0505)	2.0170 (2.0893)
	2.0294	2.3157	2.0238	2.0472	2.0086	2.1319	2.0501 (2.1492)	2.0368 (2.1383)
Li–Li	3.1135	2.9701	3.1020	2.9961	2.6370	2.7562	2.6744 (2.6744)	2.6996 (2.6996)
	3.1135	3.1293	3.1020	2.9961	3.1644	3.1250	2.9809 (2.9809)	2.9867 (2.9867)
Mn–O	2.0848	1.8182	2.0840	2.0320	2.0766	2.0037	2.0499	2.0121
	2.0848	1.9421	2.0840	2.0320	2.0766	2.0037	2.0574	2.0232
	2.0896	1.9421	2.0917	2.0998	2.0984	2.0546	2.0614	2.0237
	2.1114	2.1481	2.1151	2.1040	2.1122	2.3136	2.1204	2.0912
Si–O	1.6537	1.6914	1.6520	1.5904	1.6524	1.5780	1.6480	1.6476
	1.6559	1.6914	1.6553	1.6497	1.6524	1.6035	1.6550	1.6538
	1.6559	1.7476	1.6553	1.6497	1.6549	1.6035	1.6565	1.6575
	1.6654	1.8058	1.6673	1.6780	1.6660	1.7622	1.6643	1.6577

^a Initial model is for $\text{Li}_2\text{FeSiO}_4$.**Figure 3.** Calculated total energy vs volume curves of the $\text{Li}_2\text{MnSiO}_4$ polymorphs; $Pmn2_1$ (red), $Pmnb$ (blue), and $P2_1/n$ (green). Symbols correspond to the DFT calculated data, and lines show the fitting to the Murnaghan equation of state.

Experimental. $\text{Li}_2\text{MnSiO}_4$ was prepared by dispersing 6 nm size SiO_2 particles (Cab-osil M5) in water and stabilizing them by citric acid (Aldrich). LiNO_3 and Mn-acetate (both Aldrich) were used as a source for lithium and manganese. The suspension was dried, grinded with mortar and pestle and calcinated in the reductive atmosphere ($\text{Ar} + 5 \text{ wt } \% \text{ H}_2$). The dry and grinded sample was slowly heated ($2^\circ\text{C}/\text{min}$) to 900°C ; after 10 h at 900°C , the sample was cooled to room temperature with a cooling rate of $2^\circ\text{C}/\text{min}$. As-prepared $\text{Li}_2\text{MnSiO}_4$ sample was subjected to high-temperature, high-pressure treatment in a belt-type press (hydrostatic pressure).

Different conditions were applied, with pressure in the range 2–8 GPa and temperature between 600 – 900°C . After 1 h of HP/HT treatment, the anvils were quenched to ambient conditions.

The X-ray powder diffraction patterns (XRDP) of all the samples were collected on a PANalytical X'pert PRO MPD diffractometer using $\text{Cu K}\alpha_1$ radiation ($\lambda = 1.54056 \text{ \AA}$) in a reflection geometry. The data were collected in the 2θ range between 15 and 140° in steps of 0.017° . A more detailed XRD characterization for the initial sample and the HP- $\text{Li}_2\text{MnSiO}_4$ sample obtained at 6 GPa and 600°C was performed using a STOE diffractometer operating in transmission geometry with $\text{Mo K}\alpha_1$ radiation ($\lambda = 0.70926 \text{ \AA}$). Data collection was done in a 2θ range 2 – 55° , with step size of 0.01° . The treatment of XRD patterns was carried out using the FullProf program.²⁷

A Tecnai F20 ST transmission electron microscope was used to conduct a selected area electron diffraction (SAED) characterization of the as prepared $\text{Li}_2\text{MnSiO}_4$. Microstructure of samples were observed and analyzed with a field emission scanning electron microscope (FE-SEM, Supra 35 VP, Carl Zeiss, Germany) at an accelerating voltage of 1 kV and working distance 3–4 mm by using an in-lens detector. ^6Li magic-angle spinning (MAS) NMR spectra were recorded on a 600 MHz Varian NMR system, operating at ^6Li Larmor frequency of 88.274 MHz, with rotation synchronized Hahn-echo pulse sequence. Sample rotation frequency was 15 kHz, repetition delay between consecutive scans was 0.3 s, and the number of scans was 50,000. Frequency axis in parts per million is reported relative to the lithium signal of 1 M solution of LiCl .

Results

(a) Computational Analysis of Possible Polymorphs. Li_3PO_4 . Table 1 compares the calculated lattice parameters for the fully relaxed structures of β - and γ - Li_3PO_4 with the experimental reported values. The GGA method allows a correct reproduction of the cell parameters, with an over-

(25) Morgan, D.; Curtarolo, S.; Ceder, G.; <http://burgaz.mit.edu/PUBLICATIONS/codes.php>(26) Spek, A. L. *J. Appl. Cryst.* **2003**, *36*, 7–13.

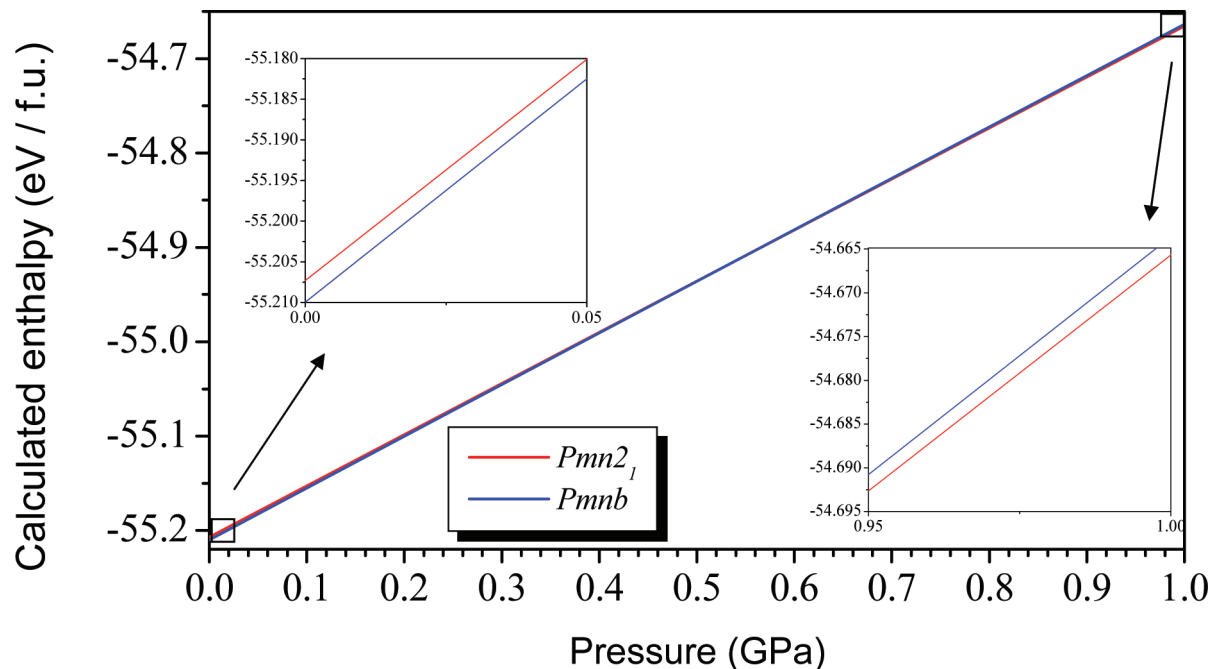


Figure 4. Calculated enthalpy vs pressure for the $\text{Li}_2\text{MnSiO}_4$ polymorphs; $Pmn2_1$ (red) and $Pmnb$ (blue).

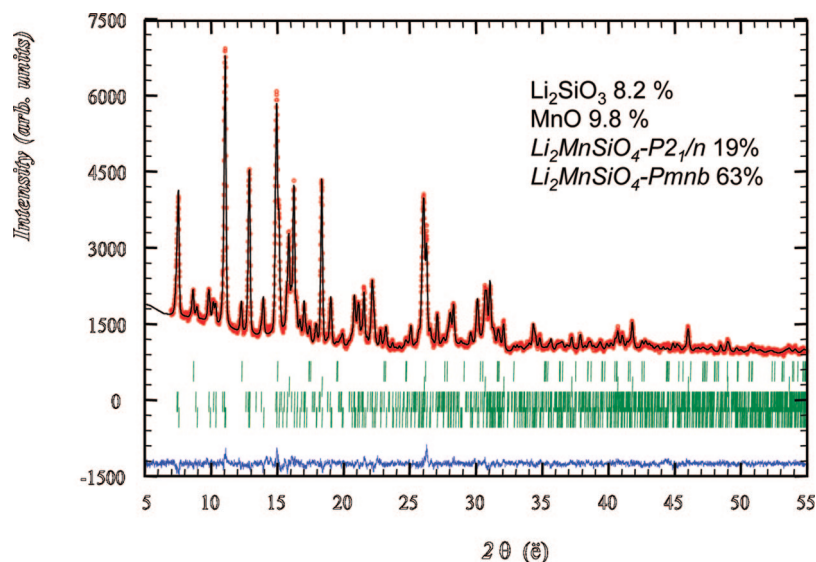


Figure 5. Observed and calculated XRD patterns of as-prepared $\text{Li}_2\text{MnSiO}_4$ ($R_p = 2.38$, $R_{wp} = 3.01$). Red profile is the observed diffractogram, black calculated, blue is the difference. Vertical bars mark reflection positions of the four phases included in the refinement; from top to bottom: Li_2SiO_3 , MnO , $P2_1/n\text{-Li}_2\text{MnSiO}_4$, and $Pmnb\text{-Li}_2\text{MnSiO}_4$. Weight fraction is indicated in the top right corner.

predictive trend that is typical for DFT methods within the GGA approximation. The LDA approximation underestimates the lattice parameters with substantially larger errors than within the GGA. It is well documented that β and γ type polymorphs of Li_3XO_4 ($X = \text{P}, \text{As}, \text{V}$) present very similar a and b lattice parameters, being the main distinction in the c lattice parameter.⁶ Noteworthy, the experimental c_γ/c_β ratio of 1.015 is nicely captured by the GGA computational method (1.016), while a larger error is found within the LDA (1.012). Thus, attending to the crystal structure reproducibility, one can say that the GGA approximation is better suited to study these structures.

Figure 2a shows the calculated total energy as a function of the volume per formula unit for $\beta\text{-Li}_3\text{PO}_4$ (black) and $\gamma\text{-Li}_3\text{PO}_4$ (violet), together with the corresponding fit of the DFT data to the Murnaghan equation of state.²⁴ As expected, the low-temperature form, $\beta\text{-Li}_3\text{PO}_4$, is energetically more stable than $\gamma\text{-Li}_3\text{PO}_4$, though the difference is small (8 meV/f.u). The energy difference within the LDA is 23 meV in favor of the $\beta\text{-Li}_3\text{PO}_4$. To produce the $\beta \rightarrow \gamma$ phase transformation, the free-energy variation of the polymorphic transformation should equal zero.

(27) Carvajal, J. R. See also a report in CPD of IUCr, Newsletter 26, (2001) 12; available at <http://www.iucr.org/iucr-top/comm/cpd/Newsletters.1993.55>

$$\Delta G_r = \Delta E_r + P\Delta V_r - T\Delta S_r \quad (1)$$

Note that DFT data refer to 0 K ($-T\Delta S = 0$). Figure 2b shows the calculated enthalpies ($\Delta H_r = \Delta E_r + P\Delta V_r$) for $\beta\text{-Li}_3\text{PO}_4$ and $\gamma\text{-Li}_3\text{PO}_4$ as a function of pressure. The $\beta \rightarrow \gamma$ transformation is slightly endothermic; therefore, it will occur with temperature if the entropy variation is positive ($\Delta H_r = T\Delta S_r$). This is in good agreement with experimental results, which show that $\beta\text{-Li}_3\text{PO}_4$ transforms to $\gamma\text{-Li}_3\text{PO}_4$ at 500 °C.^{5,6} The transformation is irreversible, being $\gamma\text{-Li}_3\text{PO}_4$ a metastable phase at RT.⁵ As shown in Figure 2b pressure is expected to favor the conversion of $\gamma\text{-Li}_3\text{PO}_4$ (metastable at RT) to $\beta\text{-Li}_3\text{PO}_4$. Accordingly, experiments performed in diamond anvil cells at 50 K showed that $\gamma\text{-Li}_3\text{PO}_4$ reverts into $\beta\text{-Li}_3\text{PO}_4$ at 120 kbar.²⁸ Interestingly, the calculated bulk modulus are 72.2 GPa for $\beta\text{-Li}_3\text{PO}_4$ and 71.9 for $\gamma\text{-Li}_3\text{PO}_4$, meaning they are somewhat compressible structures.

$\text{Li}_2\text{MnSiO}_4$. Table 2 compares the calculated lattice parameters for the fully relaxed crystal structures of $\text{Li}_2\text{MnSiO}_4$ polymorphs with the experimental values reported for each proposed model. Table 3 confronts selected calculated distances in the fully relaxed structures with those observed in the initial models. There is a good agreement between experimental and calculated bond lengths, with the exception of the $Pmn2_1$ -I model proposed for $\text{Li}_2\text{FeSiO}_4$.² This structure is substantially modified during the full relaxation, with the ions relocating to form an only corner-sharing network as that found in $\beta\text{-Li}_3\text{PO}_4$ (see additional information). Thus, the two Si–Li very short distances of 2.5 Å in the initial structure expand to 3.05 Å in the optimized structure, and the short Li–M distance of 2.7 to 3.09 Å. If only the cell shape and volume of the model are allowed to relax (this is, the atomic positions are frozen), the total energy rises up in 1.7 eV with respect to that of the fully relaxed structure. These features truly indicate that the crystal structure reported for $\text{Li}_2\text{FeSiO}_4$ is not a reasonable model for $\text{Li}_2\text{MnSiO}_4$.

Figure 3 shows the calculated total energy of $\text{Li}_2\text{MnSiO}_4$ as a function of the volume per formula unit for $Pmn2_1$ (red), $Pmnb$ (blue), and $P2_1/n$ (green), together with the corresponding fit of the DFT data to the Murnaghan equation of state.²⁴ The global minimum of energy corresponds to $Pmnb$, though the energy difference to the $Pmn2_1$ polymorph is of only 2.4 meV. This small difference falls in the computational error, thus one can not unambiguously state which polymorph is the ground state. However, at temperatures above 0 K one can expect that the softer $Pmnb$ phase will be entropically stabilized over the $Pmn2_1$ (calculated bulk moduli are 83 GPa for $Pmnb$ and 85 GPa for $Pmn2_1$). In Figure 3, the energy difference between $Pmnb$ and $P2_1/n$ is greater (65 meV/f.u.). Within the pure GGA approximation, the calculated energies of the $Pmn2_1$ and the $P2_1/n$ polymorphs are 4 and 41 meV, respectively, above that of $Pmnb$. This difference between the GGA and GGA+U results suggests that introducing the Hubbard correction term has no impact on the calculated relative stability of these polymorphs. In the end, the relative stability of $\text{Li}_2\text{MnSiO}_4$ polymorphs mimics that of the Li_3PO_4 polymorphs: the

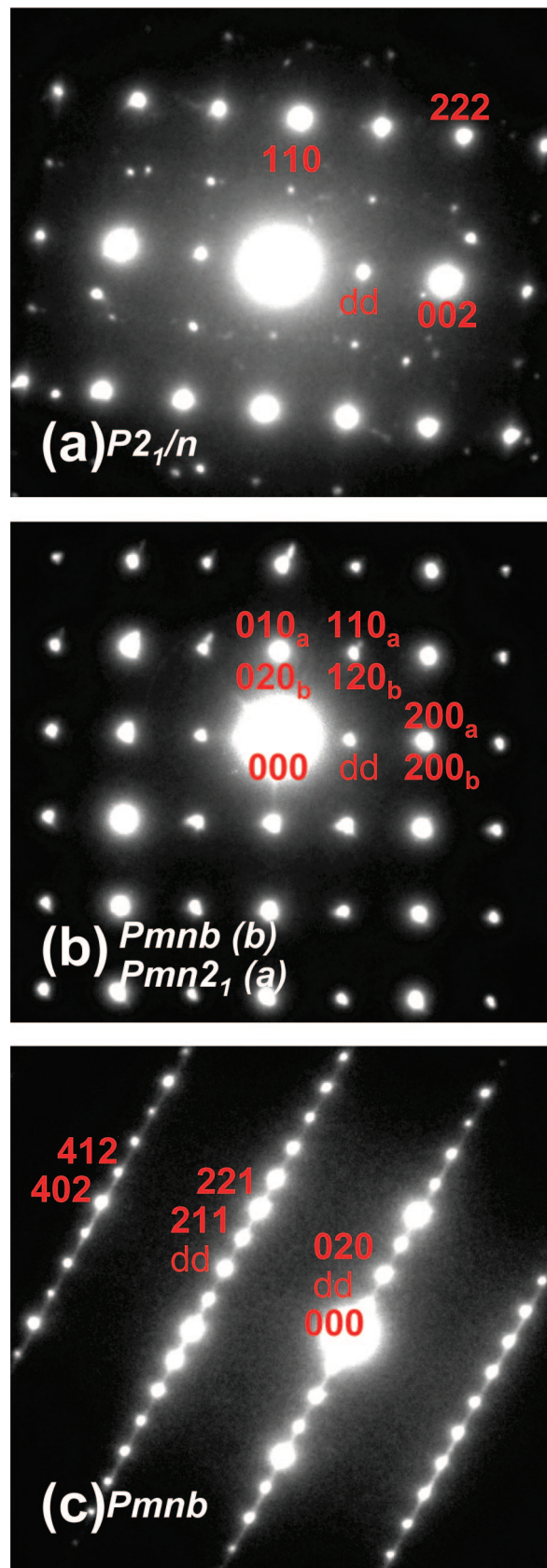


Figure 6. SAED patterns of as prepared LiMnSiO_4 sample typical of (a) $P2_1/n$ (b) $Pmnb/Pmn2_1$, and (c) $Pmnb$ polymorphs. Indexation has been done using the cell settings of Table 2. Extra spots are due to double diffraction (noted *dd* on the patterns).

crystal structures related to $\beta\text{-Li}_3\text{PO}_4$ ($Pmn2_1/Pmnb$) are more stable than the $\gamma\text{-Li}_3\text{PO}_4$ ($P2_1/n$) one. Obviously, one can not

(28) Riedener, T.; Yongrong Shen, Y.; Smith, R. J.; Bray, K. L. *Chem. Phys. Lett.* **2000**, *321*, 445.

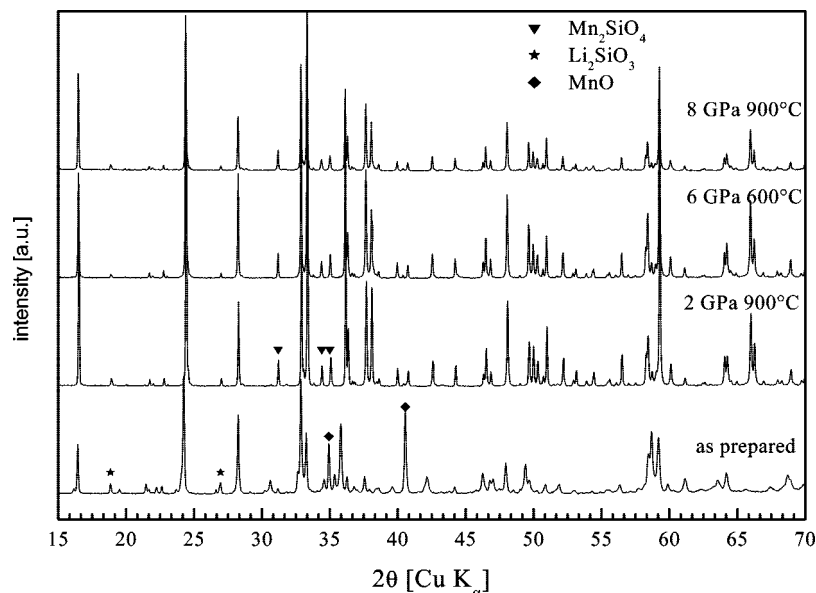


Figure 7. Comparative XRD patterns of as-prepared $\text{Li}_2\text{MnSiO}_4$ and the HP- $\text{Li}_2\text{MnSiO}_4$ obtained at different pressure–temperature conditions. Impurities are denoted by triangles (Mn_2SiO_4), asterisks (Li_2SiO_3), and diamonds (MnO).

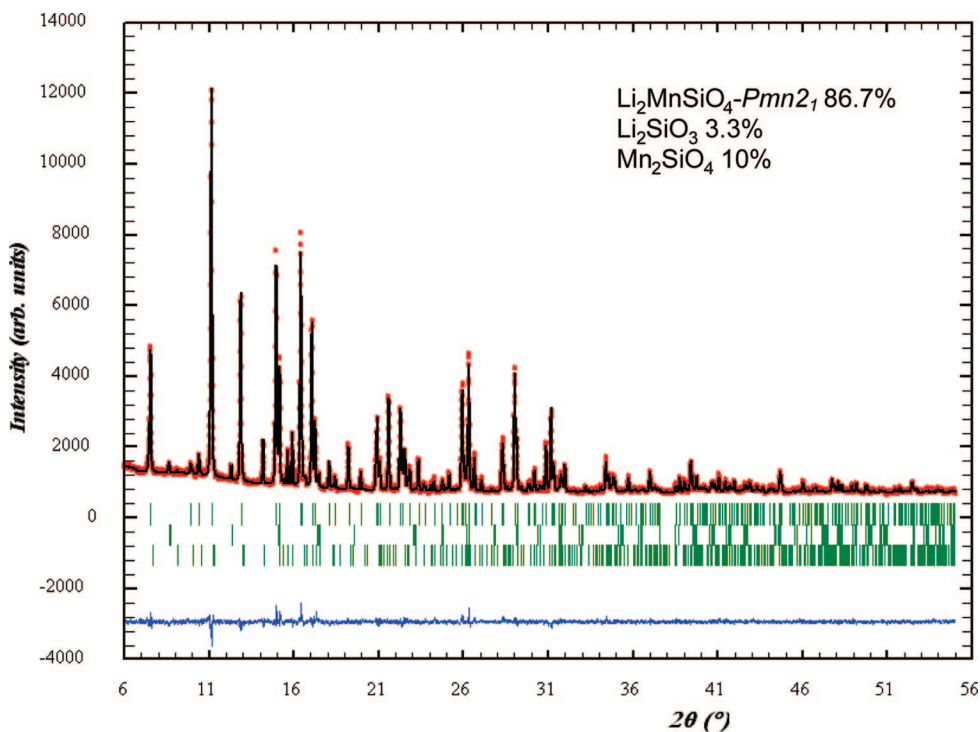


Figure 8. Observed and calculated XRD patterns corresponding to HP- $\text{Li}_2\text{MnSiO}_4$ prepared at 6 GPa and 600 °C ($R_p = 11.5\%$, $R_{wp} = 9.76\%$). Red profile is the observed diffractogram, black calculated, blue is their difference. Vertical bars mark reflection positions of the three phases included in the refinement: $Pmn2_1$ - $\text{Li}_2\text{MnSiO}_4$, top; Li_2SiO_3 , middle; and Mn_2SiO_4 , bottom. Weight fraction is indicated in the top right corner.

discard that other varieties of β - and/or γ - Li_3PO_4 than those here investigated could be energetically accessible. At this regard, Masquelier et al. prepared by hydrothermal means a $\text{Li}_2\text{MnSiO}_4$ sample whose X-Ray diffraction pattern could be indexed based on the $Pbn2_1$ cell (this is a β - Li_3PO_4 derivative).²⁹

In the view of Figure 3, the question is how to isolate each polymorph. The metastable $P2_1/n$ polymorph, which

has a larger volume than $Pmn2_1/Pmnb$, should be prepared at high temperatures and be fast quenching. This agrees well with the reported synthesis method for monoclinic $\text{Li}_2\text{MnSiO}_4$, which requires heating at 1150 °C and subsequent cooling in a few minutes.⁷ The small calculated energy difference between $Pmn2_1$ and $Pmnb$ makes it difficult to isolate any of these polymorphs by thermal treatment, in good agreement with experimental results,¹ though it might be possible adjusting both the pressure and temperature conditions of the synthesis. Figure 4 shows the calculated enthalpy vs pressure for $Pmn2_1$ and $Pmnb$ polymorphs. The denser

(29) Quoirin, G.; Dupont, L.; Taulelle, F.; Masquelier, C. Presented at the 12th International Meeting on Lithium Batteries, June 18–23, Biarritz, France, 2006; The Electrochemical Society: Pennington, NY, 2006.

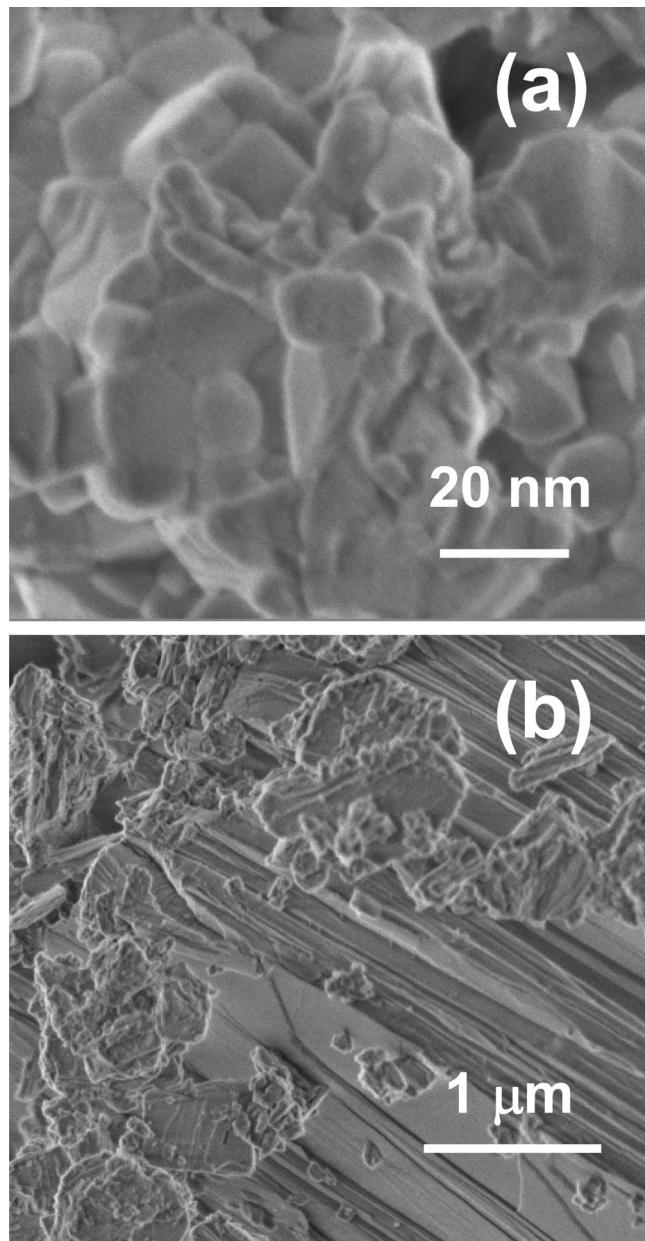


Figure 9. SEM micrographs of (a) as-prepared and (b) HP- $\text{Li}_2\text{MnSiO}_4$.

$Pmn2_1$ is certainly favored at high pressure. Thus, the strategy to isolate the $Pmn2_1$ polymorph is to apply pressure to a given $\text{Li}_2\text{MnSiO}_4$ polymorph ($P2_1/n$, $Pmnb$, or their mixtures). In the next section, this hypothesis will be experimentally verified. The $Pmnb$ polymorph might be isolated by very slow heating of the $Pmn2_1$ pure-polymorph to moderate temperatures and slow cooling down.

(b) Synthesis of Polymorphs. It has been reported that the problem of the low intrinsic conductivity of $\text{Li}_2\text{MnSiO}_4$ material can be ameliorated using small (nanosized) particles, which enable good electronic and ionic contact. Such small nanoparticles are prepared by adding carbon additives in the synthesis media. The use of small-nanosized particles, on the other hand, aggravates structural determination. In this work, contrary to previously reported synthesis routes, we have synthesized $\text{Li}_2\text{MnSiO}_4$ samples without in situ carbon and consequently the particles size exceeds 100 nm enabling a good structural determination.

The X-ray diffraction pattern of as-prepared $\text{Li}_2\text{MnSiO}_4$ sample together with its Rietveld refinement is shown in Figure 5. Crystalline impurities can be identified and indexed as MnO (ICSD-76086) and Li_2SiO_3 (ICSD-853). The pattern can be interpreted as a coexistence of $Pmnb$ and $P2_1/n$ $\text{Li}_2\text{MnSiO}_4$ polymorphs in a ratio 63:19 w/w. Refined lattice parameters for $\text{Li}_2\text{MnSiO}_4$ crystallized in $Pmnb$ S.G. are $a = 6.3126(3)$ Å, $b = 10.76567(22)$ Å, $c = 5.01183(11)$ Å, and for $\text{Li}_2\text{MnSiO}_4$ crystallized in $P2_1/n$ S.G. are $a = 6.3363(5)$ Å, $b = 10.8950(7)$ Å, $c = 5.07506(3)$ Å, $\beta = 90.99^\circ$. Introducing the $Pmn2_1$ phase into the refinement does not improve the agreement between observed and calculated patterns. However, one can not discard that some small amount of the $Pmn2_1$ polymorph is present, below a critical amount of 5%. Noteworthy, in previous experiments, a temperature of 1150 °C and quenching was needed to isolate the $P2_1/n$ polymorph,⁷ whereas a sample prepared at 700 °C and slow cooling (5 °C/min) consisted mainly on a mixture of the $Pmn2_1$ and $Pmnb$ polymorphs.¹ In the present work, at an intermediate synthesis temperature (900 °C) and slow cooling down, a mixture of $Pmnb$ and $P2_1/n$ is obtained. The compendium of these results is consistent with the calculated relative stability of polymorphs (figure 3). Furthermore, the experimental results support that the $Pmnb$ polymorph is the most stable form.

The coexistence of polymorphs in as-prepared $\text{Li}_2\text{MnSiO}_4$ has been confirmed by SAED. Some crystals display SAED patterns that can be indexed based on the monoclinic $P2_1/n$ cell (figure 6a). Most of the crystals display SAED patterns which can be interpreted according to either the $Pmn2_1$ or the $Pmnb$ cells, as shown in figure 6b (Note that the $Pmnb$ cell has double b lattice parameter with respect to the $Pmn2_1$ cell). However, there are some characteristic reflections of the $Pmnb$ -cell that are not consistent with the cell of the $Pmn2_1$ polymorph. As example, figure 6c shows a typical SAED pattern that can be indexed based on the $Pmnb$ -cell but not with the $Pmn2_1$ one.

As-prepared $\text{Li}_2\text{MnSiO}_4$ treated at 2–8 GPa and 600–900 °C results in a dark grey powder similar to that of the starting material. Figure 7 compares the XRDP of the as prepared and HP- $\text{Li}_2\text{MnSiO}_4$ samples. The HP/HT treatment produces a much more crystalline sample, even at the lower pressure used in the experiments (2 GPa). On one side HP/HT treatment reduces the amount of impurities present in the as-prepared sample (the Bragg maxima of MnO , clearly observed in the as-prepared sample, disappear), whereas new intensity peaks attributable to the formation of Mn_2SiO_4 appear. Noteworthy, the amount of Mn_2SiO_4 is larger with higher pressure and higher temperature. Independently of the pressure/temperature used in the experiments, the patterns of all the HP samples can be properly indexed based on the unit cell of $Pmn2_1$ - $\text{Li}_2\text{MnSiO}_4$. Figure 8 shows the Rietveld refinement of the HP- $\text{Li}_2\text{MnSiO}_4$ obtained at 6 GPa and 600 °C. Atomic coordinates and thermal displacement parameters were considered but only lattice parameters were refined. The amount of $\text{Li}_2\text{MnSiO}_4$ - $Pmn2_1$ (87 wt/wt %) fits to the sum of the two other polymorphs in the initial sample. The final cell parameters are $a = 6.31414(4)$ Å, $b = 5.37026(4)$ Å, and $c = 4.96503(3)$ Å. One can conclude that

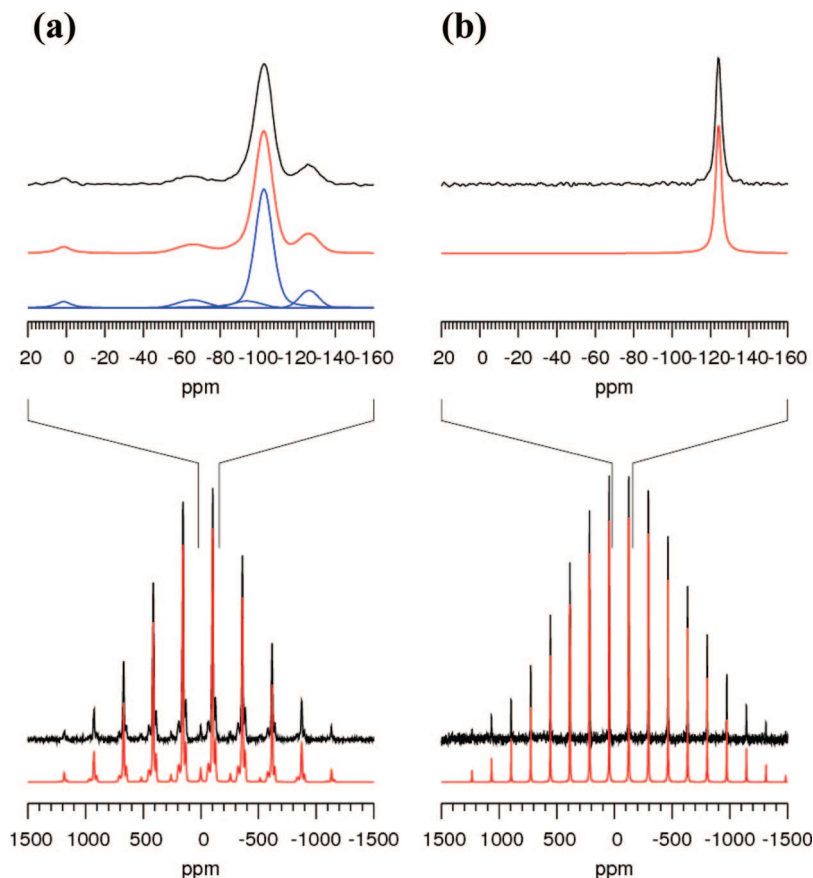


Figure 10. Patterns of spinning-sidebands (bottom) and the centerband regions (top) of ${}^6\text{Li}$ MAS NMR spectra of (a) as-prepared and (b) HP $\text{Li}_2\text{MnSiO}_4$ samples. In addition to experimental spectra (black), there are also spectra obtained after fitting (red) with individual lines belonging to three different polymorphs (blue).

Table 4. Calculated Lattice Parameters for the MnSiO_4 -Host Structures

	$Pmn2_1\text{-I}^{31}$	$Pmn2_1$	$Pmnb$	$P2_1/n$
<i>a</i>	6.172	6.175	6.172	8.454
<i>b</i>	5.704	5.690	11.508	10.141
<i>c</i>	4.851	4.869	4.859	4.840
β				93.4
<i>V</i> (f.u.)	85.40	85.56	86.28	103.58

the high pressure/high-temperature treatment allows us to fully transform the $Pmnb$ and $P2_1/n$ polymorphs into the $Pmn2_1$ one, as suggested by the first-principles calculations.

The HP/HT treatment has an influence not only on the increased purity of $\text{Li}_2\text{MnSiO}_4$ and transformation into only one polymorph but also on the particle size. The SEM micrographs of the Figure 9 show the sample morphology before and after HP/HT treatment. While as prepared $\text{Li}_2\text{MnSiO}_4$ consists of crystals of well-proportioned shape (Figure 9a), the HP- $\text{Li}_2\text{MnSiO}_4$ crystals are on average 10 μm large, built from layers that are sticking together (Figure 9b). The large crystals formed after the HP/HT treatments are not favorable for electrochemical characterization.

The differences in the crystal structure between the as-prepared and HP samples are even more pronounced in ${}^6\text{Li}$ MAS NMR spectra (Figure 10). The most intense peaks in the ${}^6\text{Li}$ NMR spectrum of $\text{Li}_2\text{MnSiO}_4$ materials can be assigned to Li nuclei that are surrounded by four Mn atoms in all three structures ($\text{Li}_{4\text{Mn}}$ nuclei). The contribution close to 0 ppm is assigned to the Li_2SiO_3 impurity as it was

determined by XRD. In the as-prepared $\text{Li}_2\text{MnSiO}_4$ sample, NMR spectra can be fitted with four different contributions (Figure 10 a). According to Rietveld refinement, the most intense line at about 102 ppm arises from the majority $Pmnb$ polymorph, whilst lines at 66 ppm and 94 ppm arises from the polymorph $P2_1/n$ (note that there are two crystallographically nonequivalent Li sites in the structure of this polymorph) and the line at 122 ppm arises from the polymorph $Pmn2_1$. The substantial difference in isotropic shifts of the three polymorphs stems from distinct Li environments in three different crystal structures (see Figure 1 and Table 3). The ${}^6\text{Li}$ NMR spectrum of the HP sample (Figure 10b) exhibits a single $\text{Li}_{4\text{Mn}}$ line at 122 ppm corresponding to the $Pmn2_1$ polymorph found in the XRD analysis. The results give strong indication for a high-pressure transformation into the metastable $Pmn2_1$ form. In addition, the line in the spectrum of the HP sample is much narrower than the lines in the spectrum of the as prepared sample, which is in agreement with higher crystallinity that is induced by high-pressure/high-temperature treatment.

(b) Influence of Crystal Structure in the Electrochemical Properties. Since 1997,³⁰ first-principles calculations have been widely used to study the electrochemical behavior of many compounds versus a lithium electrode. In the last years, the ability of the GGA+U method to precisely reproduce the electrochemical potential of a redox couple

(30) Aydinol, M. K.; Kohan, A. F.; Ceder, G.; Cho, K.; Joannopoulos, J. *Phys. Rev. B* **1997**, *56* (3), 1354–1365.

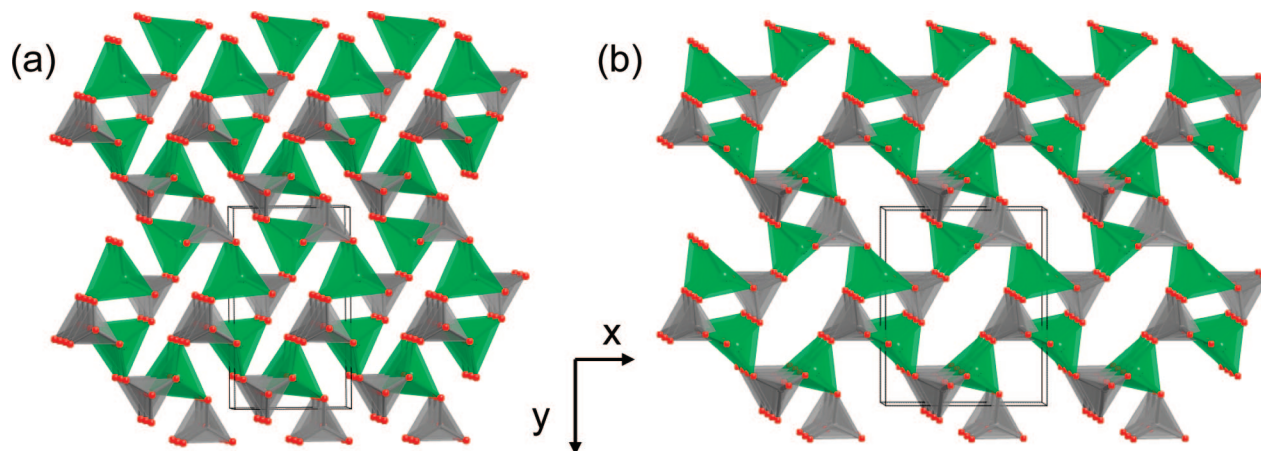


Figure 11. Optimized crystal structures of (a) $P2_1/n$ - $\text{Li}_2\text{MnSiO}_4$ (lithium ions omitted for clarity) and (b) its derivative MnSiO_4 .

has been proven for a large variety of polyoxyanionic structures and oxides.^{21,31,32} The deintercalation voltage for the first and second lithium ion from the fully relaxed $Pmn2_1$ -I $\text{Li}_2\text{MnSiO}_4$ polymorph have been predicted to be 4.13 and 4.43 V within the GGA+U approximation ($U = 6$ eV and $J = 1$ eV³¹). In the present work, in order to explore the influence of the crystal chemistry on the electrochemical properties, we have calculated the average lithium deintercalation voltage for the proposed polymorphs according to the reaction



Calculated voltages for $Pmn2_1$, $Pbmn$, and $P2_1/n$ yield 4.18, 4.19, and 4.08 V, respectively. Hence, the expected difference in the average voltage of the two-electron reaction for the γ and β hosts is only 0.1 V. This is in good agreement with the similar voltage reported for γ and β $\text{Li}_2\text{CoSiO}_4$ polymorphs.⁴ Experimentally, it is difficult to detect such a small difference when dealing with poor electronic conductor materials of large particle size, as occurs in the case of HP- $\text{Li}_2\text{MnSiO}_4$ samples (see Figure 9).

No significant difference is expected either in the electronic conductivity of the β/γ polymorphs, given that the electronic structure is governed by isolated tetrahedral MnO_4 groups in all cases. Accordingly, calculated energy gaps between the valence and conduction bands are 3.36, 3.39, and 3.2 eV for $Pmn2_1$, $Pbmn$, and $P2_1/n$, respectively. However, the lithium mobility might be quite different in the layered β ($Pmn2_1/Pbmn$) and in the three-dimensional γ ($P2_1/n$) hosts.

Table 4 lists the final lattice parameters of the optimized MnSiO_4 hosts. The fully delithiated β -type hosts (where the rigid part [MnSiO_4] is two dimensional) have slightly smaller volume than the lithiated host. The calculated volume contraction (about 1.8 %) and variation of the cell parameters under delithiation was already discussed in,³¹ where the structural instability of the $Pmn2_1$ -host was suggested. More recently, a joint computational and experimental work³³

showed that β -type hosts collapses under lithium deinsertion. The authors predicted from first principles a new structure for MnSiO_4 that is more stable than that of the delithiated $Pmn2_1$ -host. This collapsed structure (S.G. $C2/m$) is built by edge-sharing Mn^{+4} octahedra. Regarding the γ -type host, Figure 11 compares the optimized crystal structure of $P2_1/n$ - $\text{Li}_2\text{MnSiO}_4$ (lithium ions not shown) with its delithiated MnSiO_4 derivative. The framework spans a 15% in volume upon lithium removal; the a lattice parameter substantially increases (from 6.33 Å in $\text{Li}_2\text{MnSiO}_4$ to 8.45 Å in MnSiO_4) and the b parameter decreases (from 10.9 Å in $\text{Li}_2\text{MnSiO}_4$ to 10.14 Å. in MnSiO_4). From an application point of view, the γ -type host would suffer a severe structural stress upon lithium deinsertion, likely excessive to remain stable. Furthermore, using our computational settings, the collapsed $C2/m$ - $\text{Li}_2\text{MnSiO}_4$ structure proposed by Kokalj et al.³³ is 0.56 eV/f.u. more stable than the delithiated $Pmn2_1$ -host and 0.4 eV/f.u. more stable than the delithiated $P2_1/n$ -host. As the collapsed structure consists of Mn^{+4} octahedra, these total energy differences point out the strong driving force of the Mn^{+4} ions to adopt an octahedral environment, and hence the instability of the delithiated MnSiO_4 within either the γ or β structural types. Whether the instability of the ($Pmn2_1$, $Pbmn$, $P2_1/n$)- MnSiO_4 host will result in the decomposition of the material into different phases, a structural transformation, or its amorphization can not be elucidated from the available first-principles calculations data.

Conclusions

$\text{Li}_2\text{MnSiO}_4$ can adopt several crystalline forms, related to the high- (γ) and low-temperature (β) polymorphs of Li_3PO_4 . In this work, we have used DFT to guide the experiments that might be conducted to isolate each polymorph, information that is unclear solely from previous experimental reports. Calculations show that the γ - Li_3PO_4 related form (S.G. $P2_1/n$) is about 60 meV/f.u. less stable than the β - Li_3PO_4 derivatives ($Pbmn$ and $Pmn2_1$ S.G.). Because of its larger volume, the $P2_1/n$ - $\text{Li}_2\text{MnSiO}_4$ form can be prepared at high temperature and quenching. Calculated total energies of the two β - Li_3PO_4 related polymorphs differ in less than 5 meV/f.u. suggesting that it would be difficult to isolate them by means of thermal treatments. However, DFT data indicates

(31) Arroyo-de Dompablo, M. E.; Armand, M.; Tarascon, J.-M.; Amador, U. *Electrochem. Commun.* **2006**, 8 (8), 1292–1298.

(32) Le Bacq, O.; Pasturel, A.; Bengone, O. *Phys. Rev. B* **2004**, 69 (24), 245107.

(33) Kokalj, A.; Dominko, R.; Mali, G.; Meden, A.; Gaberscek, M.; Jamnik, J. *Chem. Mater.* **2007**, 198 (15), 36333640.

that high pressure will favor the formation of the $Pmn2_1$ polymorph. This has been confirmed experimentally: (i) We have prepared a $\text{Li}_2\text{MnSiO}_4$ compound that consists of a mixture of different polymorphs as detected by XRD, ^6Li MAS NMR, and SAED. (ii) Treating the as prepared sample at high pressure/high temperature allows us to isolate the $Pmn2_1$ polymorph. The temperature-driven polymorphic transformation expected for the pure $Pmn2_1$ polymorph ($Pmn2_1 \rightarrow Pmnb \rightarrow P2_1/n$) will be investigated in a forthcoming paper.

In the second part of this work, we have investigated the influence of the crystal structure on the electrochemical properties of $\text{Li}_2\text{MnSiO}_4$ as positive electrode in Li-ion cells. Calculated average lithium intercalation voltages for the two electron process are 4.18, 4.19, and 4.08 V, for $Pmn2_1$, $Pbmn$, and $P2_1/n$, respectively. All the MnSiO_4 delithiated polymorphs are predicted to decompose under lithium deinsertion. From an application point of view, having a mixture $\text{Li}_2\text{MnSiO}_4$ polymorphs or a unique $\text{Li}_2\text{MnSiO}_4$ polymorph in the electrode material seems to be a minor issue. Further

efforts should be addressed to produce a more stable delithiated- MSiO_4 if two electrons are to be reversibly intercalated in these class of silicates.

Acknowledgment. Financial resources for this research were provided by the Spanish Ministerio de Educación y Ciencia (MAT2007-62929, CSD2007-00045), Universidad Complutense/Banco Santander (PR34/071854), MEC/EGIDE (HF-2006/0026), Ministry of Education, Science and Sport of Slovenia (MNT ERA-net project), and from the European Network of Excellence 'ALISTORE'. MEAD is grateful to CIEMAT Supercomputing Centre for access to the jen50 SGI. Authors are indebted to Prof. Jean-Marie Tarascon for his invaluable help along every stage of this work. M.E.A.D. thanks T. Kokalj for kindly sharing his structural models and fruitful discussions. Comments from K. Persson, J. Thomas, C. Masquelier, U. Amador, and A. Meden are greatly appreciated.

Supporting Information Available: Additional tables and figure (PDF). This material is available free of charge via the Internet at <http://pubs.acs.org>.

CM801036K